LA-UR-18-23703
Approved for public release; distribution is unlimited.

Title: Evaluation of DNB Predictive Capability in Multiphase Boiling Model of STAR-CCM+

Author(s): Kim, Seung Jun
Baglietto, Emilio
Demarly, Etienne

Intended for: Report

Issued: 2018-04-30

Evaluation of DNB Predictive Capability in Multiphase Boiling Model of STAR-CCM+

Seung Jun Kim
Nuclear Engineering and Nonproliferation group (NEN-5)
Los Alamos National Laboratory
Los Alamos, NM 87544

Emilio Baglietto, Etienne Demarly
Nuclear Science & Engineering
MIT, Cambridge MA 02139

Executive Summary

The current milestone report is to evaluate the predictive capability of the existing boiling model in the commercial Computational Fluid Dynamics (CFD) package (so called, STAR-CCM+11.04.012), and validate the numerical calculation of a boiling curve with identification of departure from nucleate boiling (DNB) point by comparing with experimental measurements in the literatures. The current work directly demonstrates the DNB predictive capability in multiphase boiling model for nuclear reactor applications, which is tightly coupled with the CASL mission goal and evolving need from the nuclear industry. The boiling model tested here is based on the heat flux partitioning RPI approach (so called Generation-I boiling model in STAR-CCM+). A traditional experimental DNB test with a vertical pipe flow performed by Argonne National Laboratory (ANL), and a realistic 5x5-bundle fuel bundle with non-mixing vane DNB test conducted by Westinghouse Electric Company (WEC) are selected as reference experimental measurement. A baseline DNB simulation methodology is reported and its predictive capability is evaluated qualitatively as well as quantitatively with existing experiments. A parametric study of the microscopic boiling closure relations is investigated. For the pipe flow DNB validation study, the calculated DNB from the current study demonstrates good agreement with measured DNB data. The maximum deviation is observed less than 20%. The trend behaviors of DNB in varying operating conditions are similar with the observation reported in the literature. In addition, a meshing strategy for 5x5 bundle case is reported, some challenges on 5x5 bundle DNB model are also discussed. The current study provide a fundamental insight on the usefulness and limitations of the generation-I boiling model approach and may contribute to an advanced boiling model development for a practical nuclear thermal hydraulic application.

Contents

Executive Summary 1
1. Introduction 3
2. Numerical Approach of Multiphase Subcooled Flow Boiling 4
3. Selected experimental DNB tests for model Validation 6
3.1 Vertical pipe flow DNB tests by ANL (1958) 6
3.2 5x5 fuel bundle with non-mixing vane grids DNB tests by WEC (1980's) 7
4. Results and Discussions 8
4.1. Boiling curves generation using the proposed simulation protocol 9
4.2. Qualitative DNB trend behavior and quantitative DNB predictive capability 14
4.3. Meshing strategy for 5x5 bundle with non-mixing vane geometry 16
5. Conclusions and Future works 18
6. References 19

Figures

Figure 1 DNB validation studies with two different experimental tests. 6
Figure 2 Axial Geometry of Non-Mixing Vane Grid 5x5 fuel bundle CHF test [11]. 8
Figure 3 A logical path of the DNB calculation in multiphase CFD model 10
Figure 4 Mesh of the CFD model (a), void fraction distribution (b) and temperature distribution (c) at 90% of CHF condition. 11
Figure 5 Wall temperature behavior as the applied heat flux increases up to DNB point (where temperature excursion is observed in CFD). 12
Figure 6 Simulated boiling curve with DNB generated from multiphase CFD. 12
Figure 7 boiling closure characteristics with different mass flux and subcooled conditions 13
Figure 8 Comparison of the DNB trend behavior with varying conditions (close dots with solid lines are experimental results, open dots with dotted lines are CFD predictions 14
Figure 9 Calculated boiling curves with 10, 20, and 40K subcooled at three mass flux tests. 15
Figure 10 Calculated CHF compared to measured CHF at the corresponding test conditions. 16
Figure 11 5x5 fuel bundle with spacer grids (left) and a closer look on rod configuration (right). 17
Figure 12 closer look on spacer grid mesh, and preliminary conjugate heat transfer results 18

Tables

Table 1. Multiphase interaction model used in the DNB modeling study 6
Table 2. The experimental DNB datasets for comparison selected from the 1958 ANL data 7

1. Introduction

Subcooled flow boiling is a high heat transfer mode and is an excellent mechanism for heat removal in many thermal applications. However, excess vapor generation and bubble coalescence can form a thin film vapor along the heated surface, either locally or globally, leading to the condition referred to as Departure from Nucleate Boiling (DNB). DNB leads to reduced heat transfer due to the lower thermal conductivity of the vapor film, resulting in abrupt temperature rise that can possibly damage the heating surface. DNB occurs when heat flux reaches a limit called Critical Heat Flux (CHF). Therefore, the designs of heat transfer systems that operate in the subcooled boiling regime are limited by CHF or DNB. For instance, in nuclear reactors, margin to DNB is a key safety parameter [1]. In water-cooled nuclear reactor systems such as PWRs and BWRs, heat is transferred from the fuel pellets through cladding material to subcooled water. If nuclear reactors do not operate below the DNB point, significant temperature excursions will occur and eventually melt the fuel cladding leading to the release of radioactive material. Thus, comprehensive understanding of DNB phenomena and its physics-based predictive capability are tightly coupled with operational reactor safety.

While extensive experimental flow boiling tests have been conducted to investigate two phase boiling characteristics and DNB, detailed information on DNB behavior with a realistic sub-channel geometry at reactor operating conditions (i.e. high pressure) is remarkably limited. To address this shortage of data, some researchers have proposed semi-empirical DNB prediction correlations based on the bubble dynamics or force balance near at the heated surface and demonstrated some levels of DNB prediction capability for limited test conditions. An alternative approach is to use a detailed three-dimensional two-fluid models to resolve two-phase flow boiling scenarios. Computational Fluid Dynamic (CFD) has been used for advanced analysis and design study for various fluid and thermal applications in numerous industries. However, using multiphase CFD to study a boiling phenomenon has been considered to be too challenging in the past.

An open question in the boiling community is how a current state-of-the-art CFD model can predict the macroscopic boiling behavior (i.e. boiling curve and DNB value) for complex flow channel geometry at realistic reactor operating conditions. Recently, several advanced subcooled flow boiling models have been proposed by researchers to enhance the predictive capability of CFD codes in two phase applications. Lo [2] introduced a population balance equation method into the subcooled flow boiling model to account for non-uniform bubble size distribution in the two phase flow. Yeoh and Tu [3] proposed an improved interfacial area concentration model to accurately calculate the bubble size distribution. It is reported that those mechanistic modeling approach on the bubble dynamics is desired to understand the two phase interaction in the subcooled flow boiling application. Yun, et al. [4] applied a mechanistic bubbles size model to enhance the prediction capability of subcooled boiling flows. Baglietto [5] has proposed the development and validation of a complete second generation boiling closure, which leverages recent physical understanding and includes additional possible phenomenon like the bubble sliding effect at the heated surface.

The bubble behavior in subcooled flow boiling condition is fundamentally complicated and its dynamics are to be even more complex when the heat flux is getting close to the DNB point. It is apparent that capturing the physics of boiling at the wall and the bubble dynamics in the near wall region are challenging and their modeling require extensive research and experimental validation before being used for large scale engineering applications.

The current study demonstrates the applicability of multiphase boiling CFD for DNB prediction in reactor safety application, and establishes a baseline for comparison to support the development of boiling closures tested in the current validation study. In order to evaluate the DNB validation, we compare the results from multiphase CFD calculation incorporating a standard boiling model (i.e. Generation-I boiling model) to actual two experimental DNB measurement conducted by ANL [6] and WEC [11]. Chapter 2 describes the numerical approach of multiphase subcooled flow boiling model. Chapter 3 discusses selected experimental test conditions for the validation study. Chapter 4 reports the results of the CFD predication of DNB with corresponding experimental measurements. Finally, the summary of the DNB validation effort and the further work are summarized in the chapter 5.

2. Numerical Approach of Multiphase Subcooled Flow Boiling

A uniformly heated pipe flow boiling test was previously assessed by Baglietto and Christon [7]. A three-dimensional two-phase flow CFD model is prepared based on this earlier work. Incremental thermal equilibrium CFD analyses are conducted to calculate a full history of the boiling curve from the single phase heat transfer, nucleate boiling heat transfer, up to DNB point. The DNB simulation CFD methodology used in the current study basically follows the typical two phase flow boiling experimental approach. Thus, the full cycle of a boiling test consists of a succession of thermal equilibrium steady state calculations. The heat flux is increased step by step until the DNB is detected. The tasks for the boiling model validation can be listed as below.

The CFD simulations solve a system of conservation equations of mass, momentum, and energy for two phases with a set of heat partitioning RPI wall boiling model closures. The conservation equations for mass, momentum, and energy are listed, respectively [8]:

$$\frac{\partial(\alpha_k\rho_k)}{\partial t} + \nabla\cdot(\alpha_k\rho_k\vec{u}_k) = \Gamma_k, \tag{1}$$

$$\frac{\partial(\alpha_k\rho_k\boldsymbol{u}_k)}{\partial t} + \boldsymbol{\nabla}\cdot(\alpha_k\rho_k\boldsymbol{u}_k\boldsymbol{u}_k) = -\boldsymbol{\nabla}(\alpha_k p) + \boldsymbol{\nabla}\cdot[\alpha_k(\boldsymbol{\tau}_k + \boldsymbol{\tau}_k^T)] + \alpha_k\rho_k\boldsymbol{g} + (\boldsymbol{u}_{ki}\Gamma_k + p\boldsymbol{\nabla}\alpha_k + \boldsymbol{M}_{ik} - \boldsymbol{\nabla}\alpha_k\cdot\boldsymbol{\tau}_k), \tag{2}$$

$$\frac{\partial(\alpha_k\rho_k h_k)}{\partial t} + \boldsymbol{\nabla}\cdot(\alpha_k\rho_k h_k\boldsymbol{u}_k) = \boldsymbol{\nabla}\cdot[\alpha_k(\boldsymbol{q}_k + \boldsymbol{q}_k^T)] + \alpha_k\frac{D_k p}{Dt} + (h_{ki}\Gamma_k + q''_{ki}\alpha_i), \tag{3}$$

To capture the effects of turbulent flow, a standard Reynolds-Averaged Navier-Stokes (RANS) k-ε model was chosen with a high y+ wall function treatment. The transport equations for turbulent kinetic energy and energy dissipation rate are solved for each phase. The dispersed phase bubble flow and interactions at the interfaces between the two phases may promote or suppress turbulent effects. However, the effect of turbulence models on the DNB is not considered in the current study. Instead, we focus on wall boiling as a key component for an accurate multiphase DNB modeling. The heat transfer partitioning model [9] has been widely used in multiphase CFD applications, and is accepted as a general practice for the wall boiling model. Boiling heat transfer near the heated surface is significantly complex and chaotic, and so the heat transfer partitioning model attempts to classify the overall heat transfer into three

principal components: single-phase turbulent convection, evaporative heat transfer, and quenching heat transfer. These mechanisms are defined as

$$q_{\text{convective}} = A_1 h_c (T_w - T_f), \tag{4}$$

$$q_{\text{quenching}} = A_2 h_q (T_w - T_f), \tag{4}$$

$$q_{\text{evaporation}} = N_a f_d \left(\frac{\pi D_d^3}{6}\right) \rho_g h_{fg}), \tag{5}$$

Where, N_a indicates the active nucleation site density, D_d and f_d present the bubble departure diameter and frequency, respectively, and A_1 and A_2 are the fractions of the areas subjected convective and quenching heat transfer. The sum of A_1 and A_2 should be always unity. The value of A_2 can be defined as following equation using a bubble influence factor K:

$$A_2 = K N_a \left(\frac{\pi D_d^2}{4}\right). \tag{6}$$

In order to detect DNB, a detection criterion is used to transition heat transfer mode from a liquid phase convective heat transfer to vapor phase convective heat transfer mode.

$$q_{wall} = f \times \left(q_{convective_{liquid}} + q_{quenching} + q_{evaporation}\right) + (1 - f) \times q_{convective_{gas}} \tag{7}$$

Where, f is a function between 0 and 1 that drives the heat transfer regime. f is defined as:

$$f = \begin{cases} 0 & \alpha_\delta \le \alpha_{dry} \\ \beta^2(3 - 2\beta) & \alpha_\delta > \alpha_{dry} \end{cases} \tag{8}$$

- α_{dry}: The volume fraction threshold that represents the beginning of the DNB process and the change in heat transfer regime.
- α_δ: The vapor volume fraction averaged over the bubbly layer thickness.
- β is defined:

$$\beta = \frac{\alpha_\delta - \alpha_{dry}}{1 - \alpha_{dry}} \tag{9}$$

The commercial finite-volume based CFD code, STAR-CCM+ is used for all computations in the current calculation. Note that many commercial CFD tools for subcooled flow boiling applications provide various closure options for the wall boiling model. However, most closure models are empirical correlations based on the various pool boiling tests. Therefore, additional care is required when selecting boiling closure options in subcooled boiling applications. To improve predictive capability, rigorous parametric studies of closure models in the wall boiling is strongly recommended.

In addition, the detailed multiphase interaction models used in the current study are summarized in Table 1. The lift force is considered to be constant. The lift coefficient can be an important boiling closure for the vertical flow boiling simulation. A simple sensitivity study of the lift force on the DNB prediction is performed. Among the various lift coefficient models, the constant lift coefficient method (i.e., zero lift, etc.) shows most reasonable DNB prediction

capability. A further sensitivity study of the lift force with different flow orientations (horizontal flow or inclined/declined flow channel) should be investigated to enhance the maturity of the current boiling model practice.

Table 1. Multiphase interaction model used in the DNB modeling study

Phase interaction Boiling closure	Selected model in the current test
Drag force	Tomiyama model
Lift force	constant value with sensitivity
Wall Lubrication force	Not included
Virtual Mass	Not included
Bubble Departure frequency	Cole model
Bubble Departure diameter	Tolubinski Kostanchuk model
Nucleation site density	Lemmer Chawla model
Boiling Mass Transfer rate	Ranz-Marshall model
Bubble Induced Quenching Heat transfer coeff.	Del Valle Kenning model
Interaction Area Density method	Spherical Particle assumption
Interaction Length Scale	Kurul Podowski assumption

3. Selected experimental DNB tests for model Validation

Two different sets of experimental DNB test campaigns are selected for model validation. One is a single vertical pipe flow DNB test: a standard DNB test configuration, other case is a 5x5 fuel bundle DNB test, which represents a realistic sub-channel configuration for PWR conditions. The mentality of the DNB validation approach in the current study is to evaluate the multiphase boiling with a simple geometry with parametric boiling closure study, then extend the validation effort toward the a realistic complex fuel channel geometry with spacer grid as shown in the Figure 1

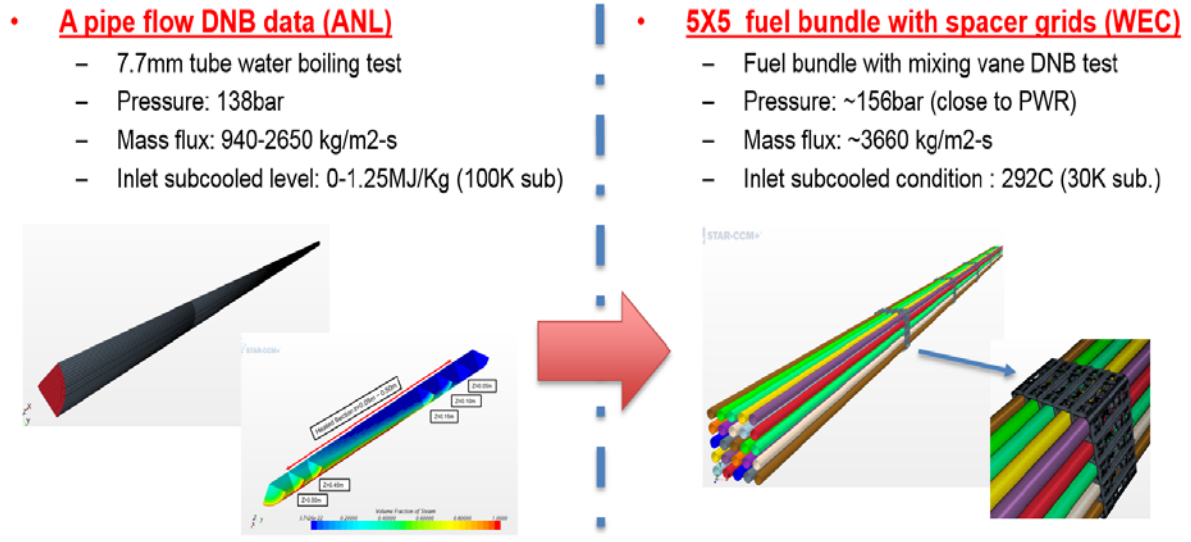

Figure 1 DNB validation studies with two different experimental tests.

3.1 Vertical pipe flow DNB tests by ANL (1958)

Experimental DNB measurements for high pressure water systems were reported by ANL [6]. These experiments were performed with varying system parameters that affect flow boiling

operating conditions. The parameters include flow channel geometry, mass flux, system pressure, inlet temperature, and calculated thermo-equilibrium exit quality based on the energy balance. It is considered that ANL's experimental DNB tests are suitable for the current DNB validation study for two reasons. First, the flow boiling condition is reasonably close to the practical PWR operating conditions. Second, the flow boiling test condition and the measured DNB are explicitly described. Among all DNB datasets, we select 48 cases from the ANL report that correspond to three mass flux groups (940, 1670, and 2650 kg/m^{2}s) with varying level of subcooled condition (0-1.25 MJ/kg). Note that the inlet subcooled temperature is calculated from the inlet subcooled enthalpy by applying thermodynamic water properties at the given system pressure (i.e. 138 bar). The 48 cases are summarized in the Table 2. Both qualitative and quantitative comparison study on the predictive capability of DNB modeling will be reported in the following section. Some of selected DNB calculation from the current study are additionally validated with the CHF look up table data at the corresponding test condition [10].

Table 2. The experimental DNB datasets for comparison selected from the 1958 ANL data.

Test	Mass Flux [Kg/m^{2}s]	subcooled enthalpy [J/kg]	DNB [MW/m^2]	Test	Mass Flux [Kg/m^{2}s]	subcooled enthalpy [J/kg]	DNB [MW/m^2]
1	963	1265344	4.038	25	1614	90714	1.571
2	956	939704	3.155	26	1668	995528	5.174
3	932	695474	2.713	27	1655	828056	4.480
4	926	502416	2.271	28	1668	721060	4.069
5	913	260512	1.719	29	1668	595456	3.596
6	913	159331	1.514	30	1682	481482	3.155
7	936	98855	1.369	31	1682	351226	2.650
8	936	1295582	4.069	32	1682	260512	2.256
9	956	1137414	3.596	33	2563	695474	5.363
10	943	946682	3.155	34	2618	518698	4.480
11	929	711756	2.713	35	2712	427984	4.069
12	925	483808	2.230	36	2672	360530	3.596
13	929	276794	1.798	37	2645	274468	3.139
14	929	159331	1.530	38	2590	211666	2.697
15	944	98855	1.360	39	2550	146538	2.271
16	890	23260	1.218	40	2618	62802	1.830
17	1668	990876	5.205	41	2645	660584	5.268
18	1655	807122	4.322	42	2645	514046	4.543
19	1655	737342	4.069	43	2699	395420	3.880
20	1736	583826	3.628	44	2685	360530	3.596
21	1695	458222	3.091	45	2658	276794	3.155
22	1682	351226	2.650	46	2604	223296	2.729
23	1682	272142	2.334	47	2563	144212	2.256
24	1655	172124	1.877	48	2658	65128	1.798

3.2 5x5 fuel bundle with non-mixing vane grids DNB tests by WEC (1980's)

A 5x5 rod bundle CHF test was conducted on a brazed Inconel non-mixing vane grid design at the Columbia University's Heat Transfer Research Facility in the 1980's [11]. The test section simulates a 5x5 fuel bundle array (e.g. 6 hot rods and 19 cold rods) with 5 non-mixing vane

spacer with 21.5-inch grid spacing configuration. The detailed geometry and dimension of non-mixing vane spacer grid are not included in this report due to the WEC's proprietary design information. The schematic diagram of the axial location of the full scale test configuration for the DNB test is demonstrated in Figure 2. The DNB test matrix was designed to cover a representative PWR operating conditions (100 bar < pressure < 165 bar, 1000 kg/m2-s < mass flux < 7000 kg/m2-s, inlet subcooled level range: 5 ~ 100 C).

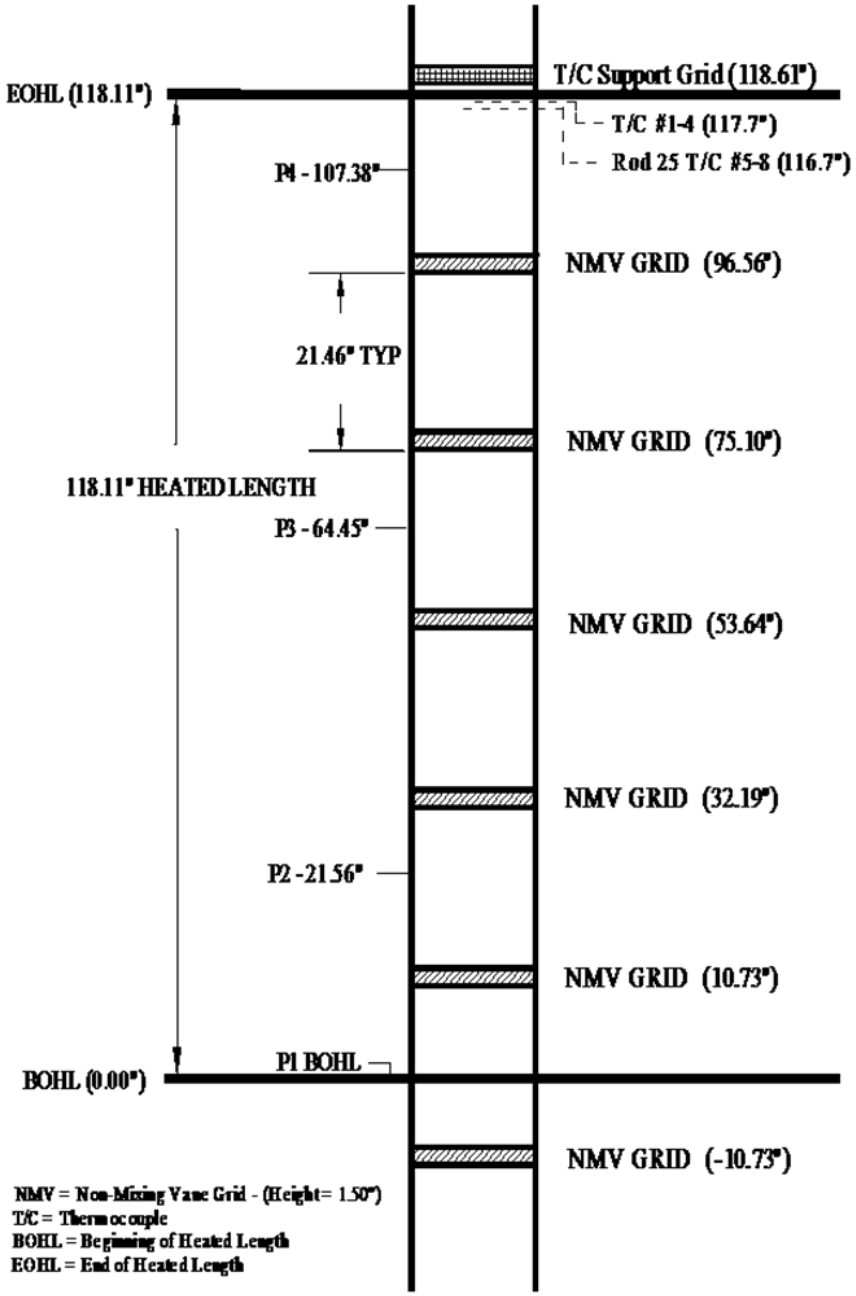

Figure 2 Axial Geometry of Non-Mixing Vane Grid 5x5 fuel bundle CHF test [11].

4. Results and Discussions

The DNB simulation methodology and preliminary results from the current study are reported here. For the vertical pipe flow DNB test, we compared the predicted DNB value from CFD

with experimental measurements qualitatively and quantitatively. The validity of the DNB model for the pipe flow application is assessed by conducting the boiling closure parametric study. In addition, a 5x5 fuel bundle meshing strategy is reported and some challenges on fuel bundle DNB meshing and modeling are also discussed.

4.1. Boiling curves generation using the proposed simulation protocol

The CFD model domain represents the exact geometry in the test configuration of ANL's experiments. Using symmetry, the CFD domain is only modeled in ¼ of the pipe geometry by implementing the symmetry boundary condition, which enables the model inexpensive in term of computing cost without loss of physics. The hexahedral-dominant mesh shown in Figure 4 is used in the CFD model. The total number of cells in the mesh is approximately 0.4 million. The base size of 0.2 mm was chosen with 2 layers of prism mesh next to the heated wall. The near wall mesh is treated with a prism mesh with total thickness of 0.5 mm, resulting in a y^+ value larger than 30 throughout most of the flow. The high y^+ wall treatment of the k-ε turbulence model is used in the current study. A mesh sensitivity study on the boundary layer and bulk flow region was performed. The criterion for onset of DNB is that the void fraction at the wall reached 90% at $y^+ = 200$[5].

The length of the heated section is 47.5 cm with two extensions of 10 cm unheated zone before and after the heated section. The uniform heat flux is applied on the heated wall surface along with flow direction. The boundary condition for inlet is defined as a fully developed pipe flow profile with a fixed temperature, and the outlet is set to a pressure-out condition. The fully developed inlet velocity distribution is calculated and applied into the inlet boundary condition by using a field function. Initializing the inlet from this fully-developed flow condition helps to reduce the entrance zone mesh count and accelerate the simulation.

Some characteristic results in which the heat flux is set to 90% of CHF are presented below. The void fraction distribution along the heated channel is shown in Figure 4(a). The local temperature is also reported in Figure 4(b). The calculation of temperature and the volume fraction of the steam profile at certain heat flux allow insight where the potential DNB location would occur in the pipe. The applied heat flux is increased in 0.05 MW/m^2 increments. The thermal equilibrium condition at a given heat flux condition is archived by monitoring wall temperature. By iterating this procedure, a boiling curve with identification of DNB point is generated as illustrated in Figure 3. The DNB point is characterized by an abrupt increase in wall temperature, which is identical DNB identification criterion in the experimental boiling test. An example of the wall superheated temperature monitoring over the whole simulation process s is shown in Figure 5. The wall superheated temperature is monitored near at the outlet region as the applied heat flux incrementally increases.

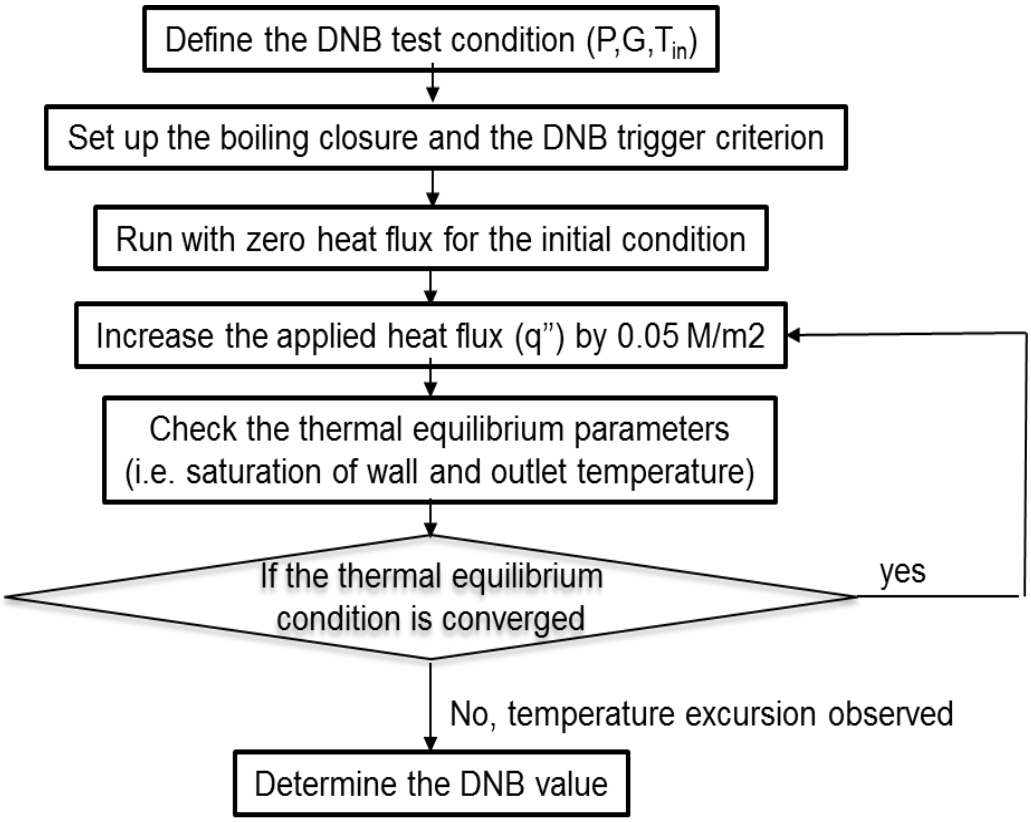

Figure 3 A logical path of the DNB calculation in multiphase CFD model.

The behavior of wall temperature in the boiling simulation represents three modes of heat transfer: single-phase heat transfer, nucleate boiling heat transfer, and DNB. The temperature excursion takes place near at the heat flux of 1.9MW/m^2. For applied heat flux greater than 1.9MW/m^2, the wall temperature does not converge and CFD simulation becomes very unstable even though the simulation runs for sufficient iterations.

Figure 5 can be replotted into a typical boiling curve with heat flux of a vertical axis and superheated wall temperature in horizontal axis as shown in Figure 6. The calculated boiling curve also notably demonstrate two different heat transfer modes. At low heat flux (i.e. below 25% of CHF) the primary boiling mechanism near the wall is found to be single phase heat transfer mode. As expected and observed from other literatures, the heat transfer coefficient in this regime is relatively low since the nucleate boiling has not triggered yet. As heat flux increase, where the wall superheat temperature is close to around 5°C, the heat transfer mode transitions to nucleate boiling. In this regime, the heat transfer coefficient, which is the gradient of the boiling curve, notably improved as a factor of seven time larger than the single-phase heat transfer coefficient. Afterward, the calculated boiling curve indicates a region where the boiling heat transfer mechanism is slight reduced, and then finally the DNB is detected, where a rapid temperature excursion takes place in the simulation.

(a)

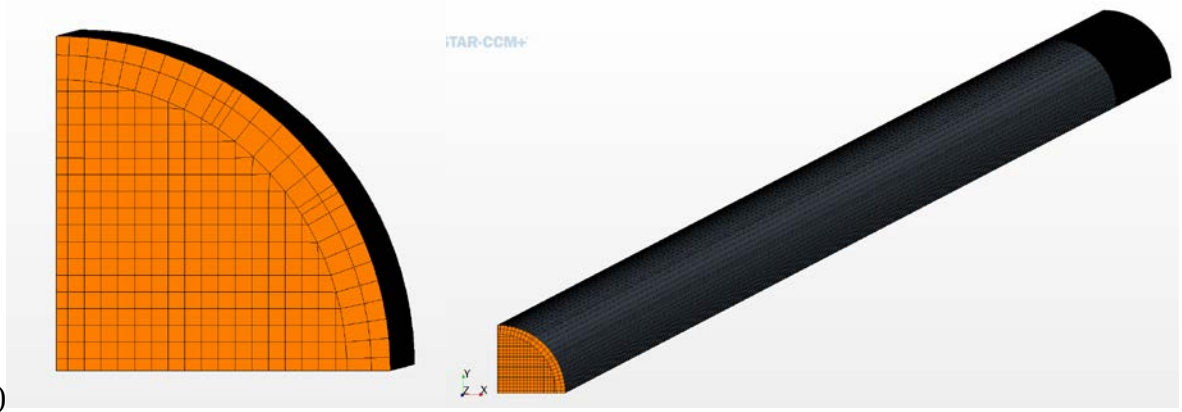

(b)

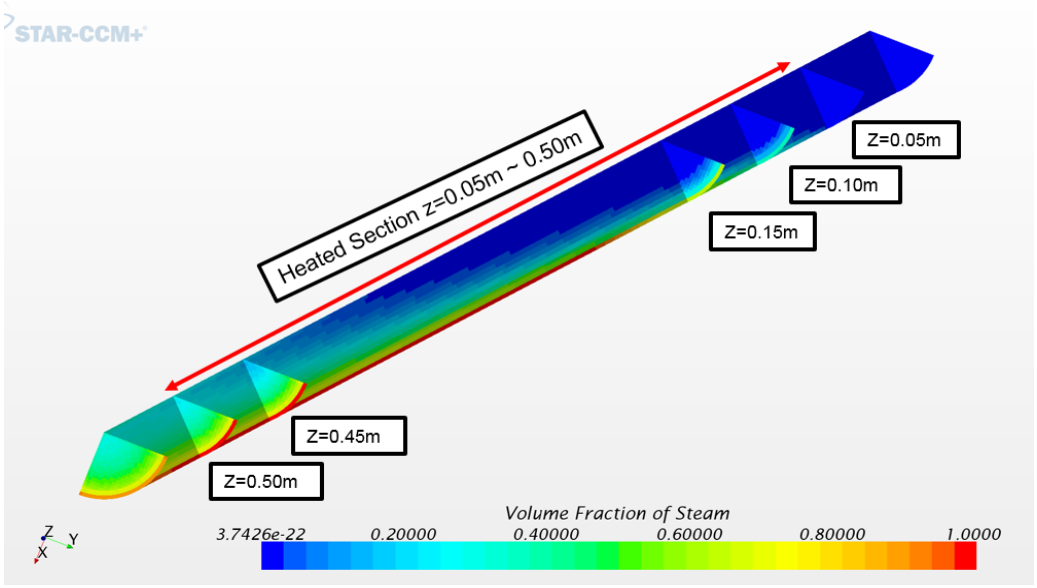

(c)

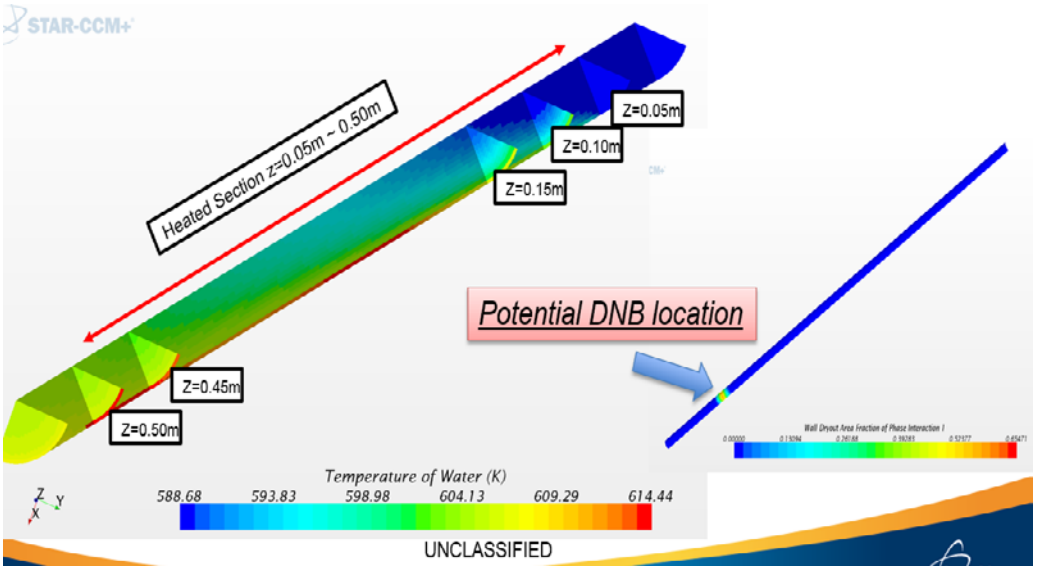

Figure 4 Mesh of the CFD model (a), void fraction distribution (b) and temperature distribution (c) at 90% of CHF condition.

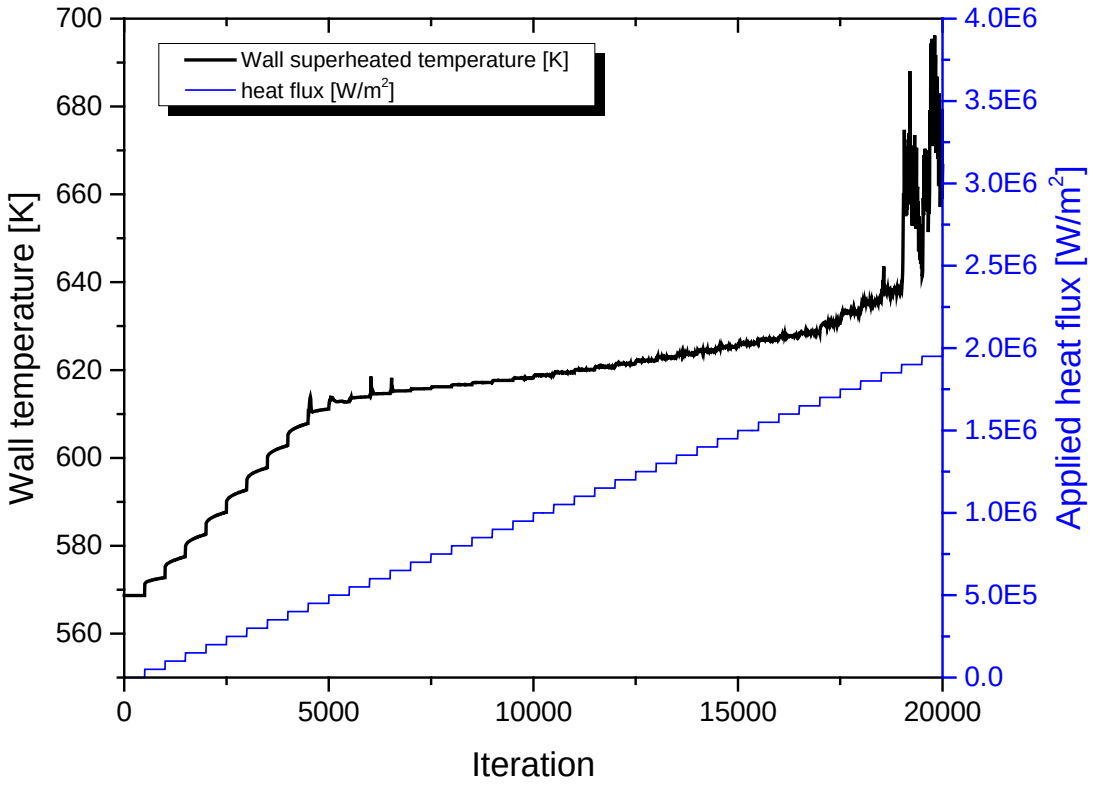

Figure 5 Wall temperature behavior as the applied heat flux increases up to DNB point (where temperature excursion is observed in CFD).

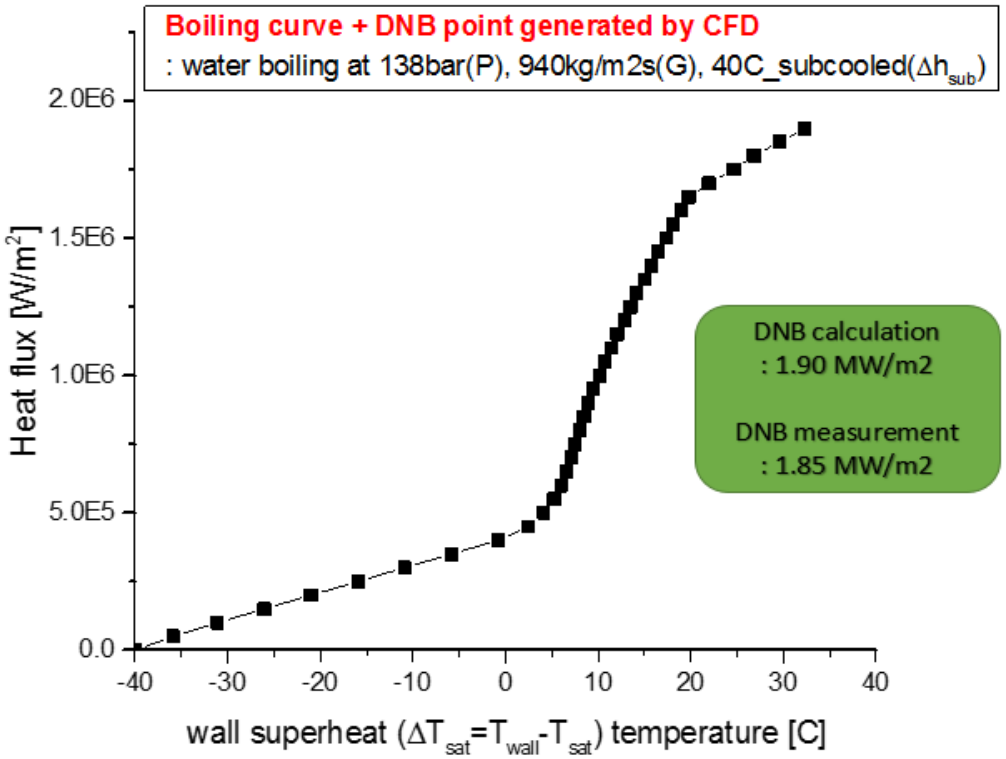

Figure 6 Simulated boiling curve with DNB generated from multiphase CFD.

In the nucleate boiling regime, boiling closures parameters related to the evaporation term become crucial. The behaviors of microscopic parameters (i.e. bubble departure diameter, bubble departure frequency, and nucleate site density) with respect to mass flux and subcooled level are shown in Figure 7. Bubble departure diameter is found to decrease with increasing mass flux and increasing subcooled level. Bubble departure frequency is found to increase with increasing mass flux as well as increasing subcooled level. Those observations are consistent with experimental boiling heat transfer literatures [7]. Nucleation site density seems to be less susceptible to the mass flux and subcooled condition. A sensitivity of boiling closure on the DNB simulation is an important open question, and further investigation on the boiling closure model is highly recommended to improve the accuracy and robustness of DNB model.

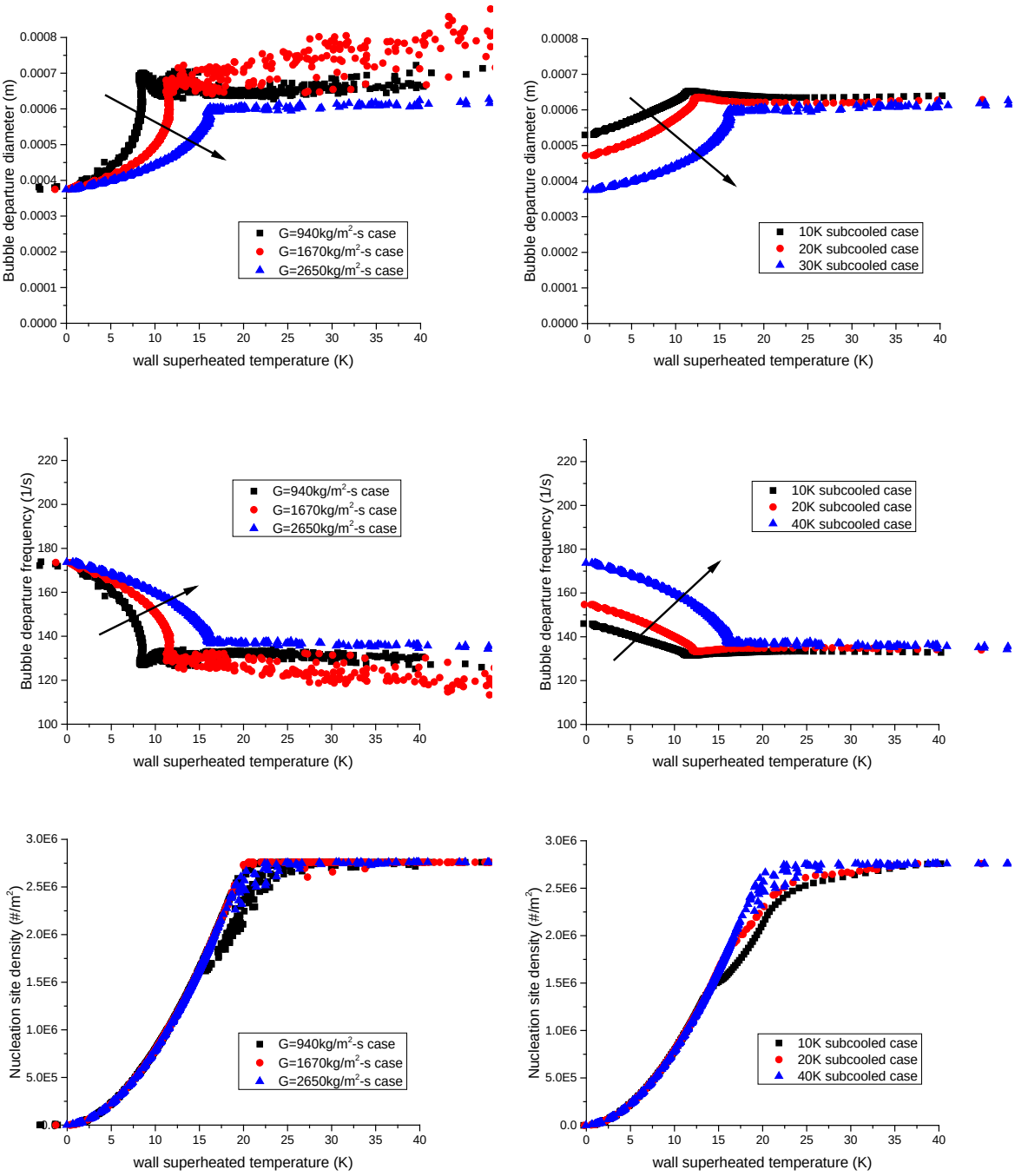

Figure 7 boiling closure characteristics with different mass flux and subcooled conditions.

4.2. Qualitative DNB trend behavior and quantitative DNB predictive capability

The development of a baseline DNB simulation method with some level of parametric studies are finished, an extended DNB test matrix is performed with various operating conditions. In order to validate the current boiling model in a wide range of operating condition, three groups of test condition are selected. Each group has constant mass flux (e.g. 940 kg/m^{2}s, 1670 kg/m^{2}s, 2650 kg/m^{2}s) with varying inlet fluid temperatures (e.g. 10°C, 20°C, 40°C, 70°C, and 100°C subcooled level). The total number of boiling test conducted in this study is 15. In this extended DNB validation study, two main aspects are closely evaluated.

- Qualitative trend behavior of DNB with varying system parameters (i.e. the effect of subcooled level on DNB, the effect of mass flux on DNB)
- Quantitative DNB prediction accuracy by comparing with corresponding datasets

Based on the best practice guideline (BPG) that we demonstrated here, all tests follow the same CFD methodology to calculate a full story of boiling curve up to the DNB point. Among the three mass flux groups, a group of mass flux of 2650 kg/m^{2}s show most accurate trend compared to low (940 kg/m^{2}s) and medium (1670 kg/m^{2}s) mass flux group. In addition the DNB prediction at high subcooled flow boiling (e.g. 70-100K subcooled conditions) is relatively poor compared to low subcooled flow boiling cases (e.g. 10-40K subcooled conditions) as shown in the Figure 8. General observations from qualitative trend behavior of DNB calculated by CFD can be summarized as follows.

- The predicted CHF value increases linearly as the inlet subcooled level increases
- The predicted CHF value increases linearly as the mass flux increases

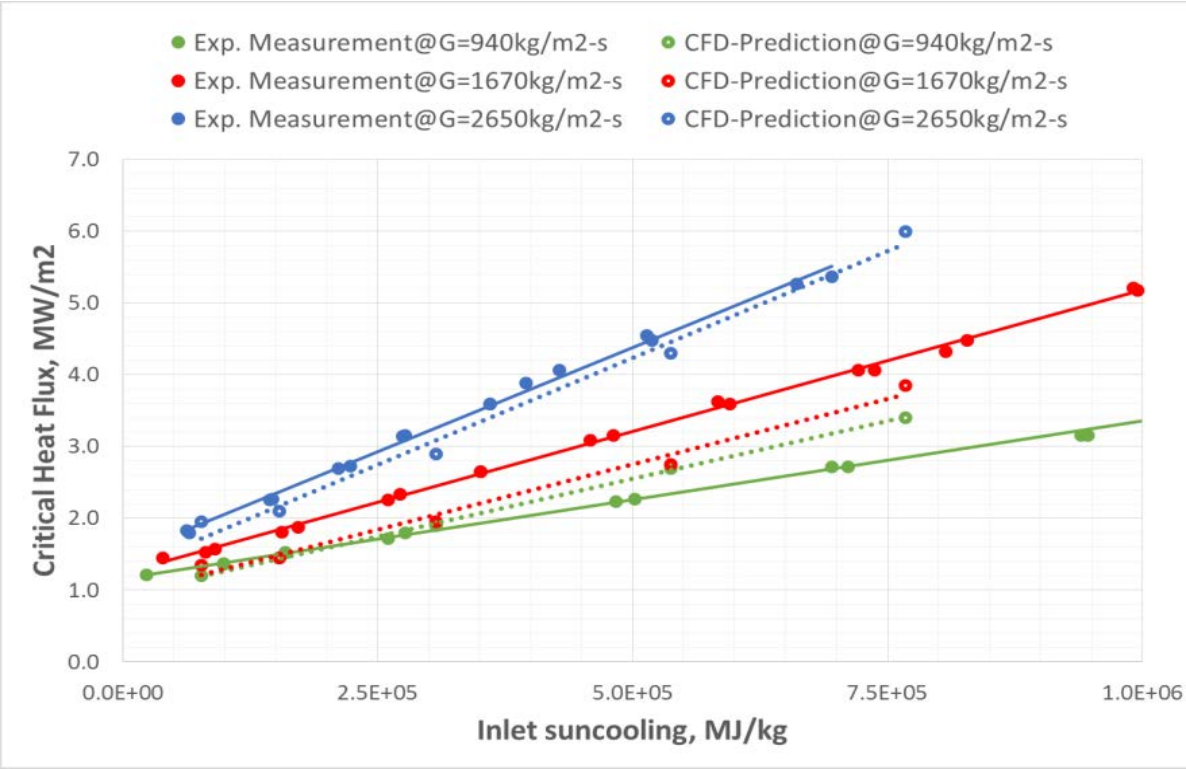

Figure 8 Comparison of the DNB trend behavior with varying conditions (close dots with solid lines are experimental results, open dots with dotted lines are CFD predictions.

Those trend behaviors observed in the current simulation study are also found in previous literatures [1, 6]. It is worth noting that most accurate DNB prediction is obtained at high mass flux with low subcooled flow condition in this study. A definitive conclusion cannot be made at this point, but turbulence model effect on the boiling closure models and evaluation of quenching term in the wall boiling model should be further investigated to extend the feasibility of the current boiling practice in a wide range of the test condition.

Figure 9 shows the calculated boiling curves up to the DNB points at each test condition grouping by the mass flux. As mentioned earlier, the DNB trend with varying system conditions (i.e. mass flux, subcooled level) is also found in these boiling curve plots here.

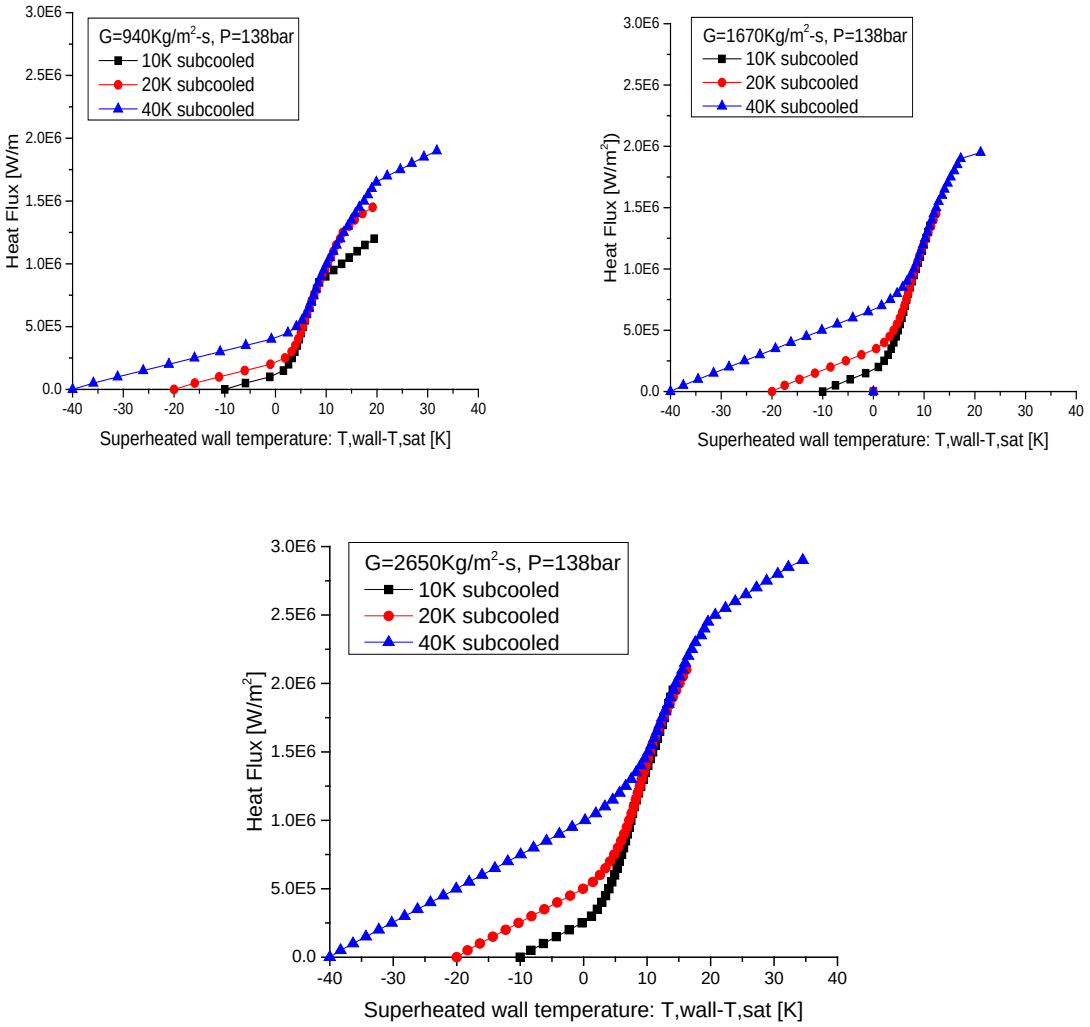

Figure 9 Calculated boiling curves with 10, 20, and 40K subcooled at three mass flux tests.

A quantitative comparison of calculated DNB with corresponding experimental dataset is conducted. The preliminary results shown in the Figure 10 illustrates that the calculated DNB from multiphase CFD demonstrates good agreement with experiment (less than 20% of deviation) at the given test conditions (i.e. Pressure of 138 bar, mass flux of 940~2650 kg/m2s, inlet subcooled temperature of 10-100 K). In order to evaluate the generality and maturity of the baseline boiling model for DNB application, a more case study and parametric boiling

closure evaluation should be further investigated for a wider range of operating condition. With the consideration of the complex wall boiling physics under the subcooled flow condition, it is usually accepted that the DNB model development with ~ 50% deviation is a reasonable modeling effort. While the current DNB validation work is only performed with the limited number of DNB test, the preliminary result presented in this study clearly demonstrate a promising path forward for the advanced DNB model using a multiphase CFD tool.

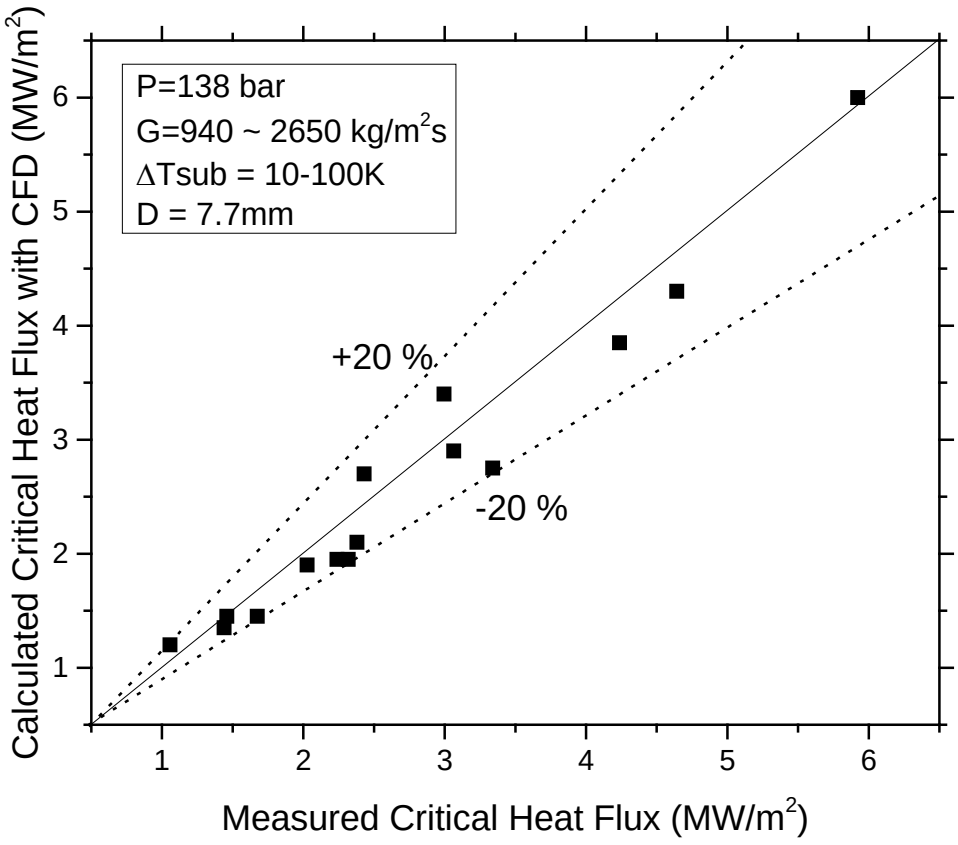

Figure 10 Calculated CHF compared to measured CHF at the corresponding test conditions.

4.3. Meshing strategy for 5x5 bundle with non-mixing vane geometry

Following the successful demonstration on the DNB prediction for pipe flow application, the DNB validation effort is extended toward more realistic geometry (i.e. 5x5 fuel bundle sub channel with spacer grids) for RWR conditions. Unlike typical single pipe flow DNB test, the industry DNB application is dealing with fuel bundle geometry with a set of spacer grids. The geometry of 5x5 bundle with non-mixing vane spacer grid case is provided from WEC to test and develop a meshing strategy for the DNB validation test.

A full length of 5x5 bundle geometry consists of 25 rods and 5 spacer-grids with non-mixing vanes. To visualize the detailed geometry of spacer grid and rod configuration, a single span quartered domain is selected as simple version of meshing test shown in Figure 11.

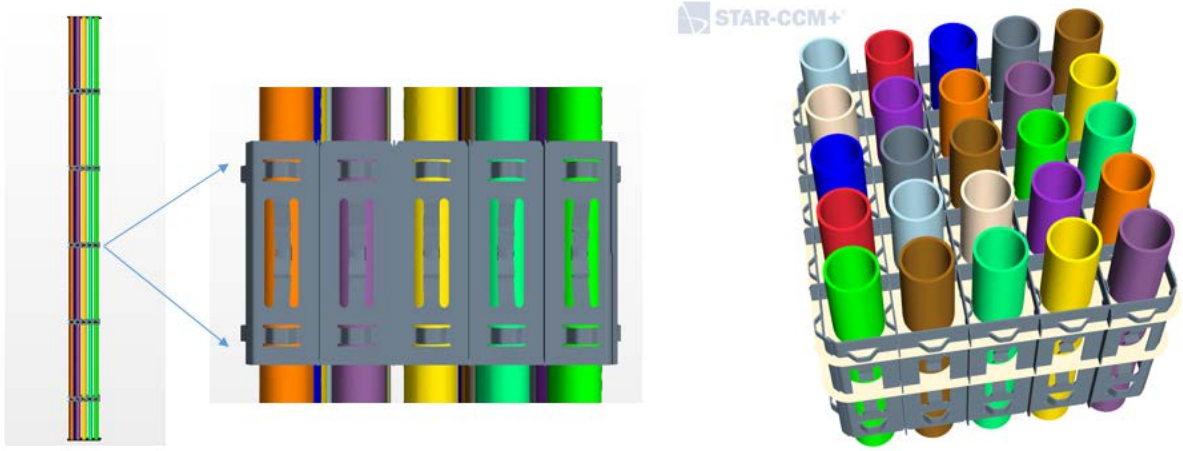

Figure 11 5x5 fuel bundle with spacer grids (left) and a closer look on rod configuration (right).

Initially, a fluid only domain approach is tested for the 5x5 bundle geometry, as it was done for previous cases. Unfortunately, this approach quickly evidenced unrealistic temperature calculation near the contact point between rods and spacer grid, due to the elimination of heat condition in the CFD model. In order to capture the correct physic in the sub channel flow, a conjugate heat transfer meshing is constructed. In this meshing, cladding and spacer-grids are meshed as part of solid domain. An evaluation test with the conjugate heat transfer modeling approach with a single span configuration is performed to evaluate if the heat generated from the rods is transporting into the spacer grid by conduction and fluid domain by convection (see the top-right picture in Figure 12). For correct conjugate model, the contacts between fluid and solid (i.e. fluid-rod, fluid-spacer grid) and solid to solid (i.e. rod-spacer grid) in the simulation have to be perfectly identified in the mesh generation. Note that the full span 5x5 bundle geometry consists of 2500 contact areas. Thus, how to manage those contact areas in the full span bundle mesh will be one of challenges in 5x5 fuel bundle DNB validation study. With a closer look on the contact between rods and spacer grid (see the bottom-left picture in Figure 12), small piece of thin sliver geometries are observed, which have been generated during the Boolean operation between the spacer and rods. It is worth noting that those very thin solid parts in the spacer grid may cause meshing issues as well as solver convergence when the multiphase model applied. Therefore, future CAD efforts could try to eliminate the problem with some level of geometry simplification to improve the robustness of the boiling model.

The thin-mesher scheme is applied on the solid parts (cladding with 6.2mm thickness, spacer grid), and the trimmer method is used for the fluid domain. The base size is set to 0.6mm, applying single prism layer on the wall boundary. For a selected single span fluid domain with mesh and preliminary conjugate heat transfer calculation results are shown in Figure 12. A uniform heat flux is applied inside of the cladding surface, and a reasonable heat transfer behavior via both conduction and convection is observed in the initial test. The lesson and learned from the current meshing study and the DNB methodology tested in a pipe flow test will be applied on the full span geometry, further investigations on the DNB validation for 5x5 bundle test will be performed in the future.

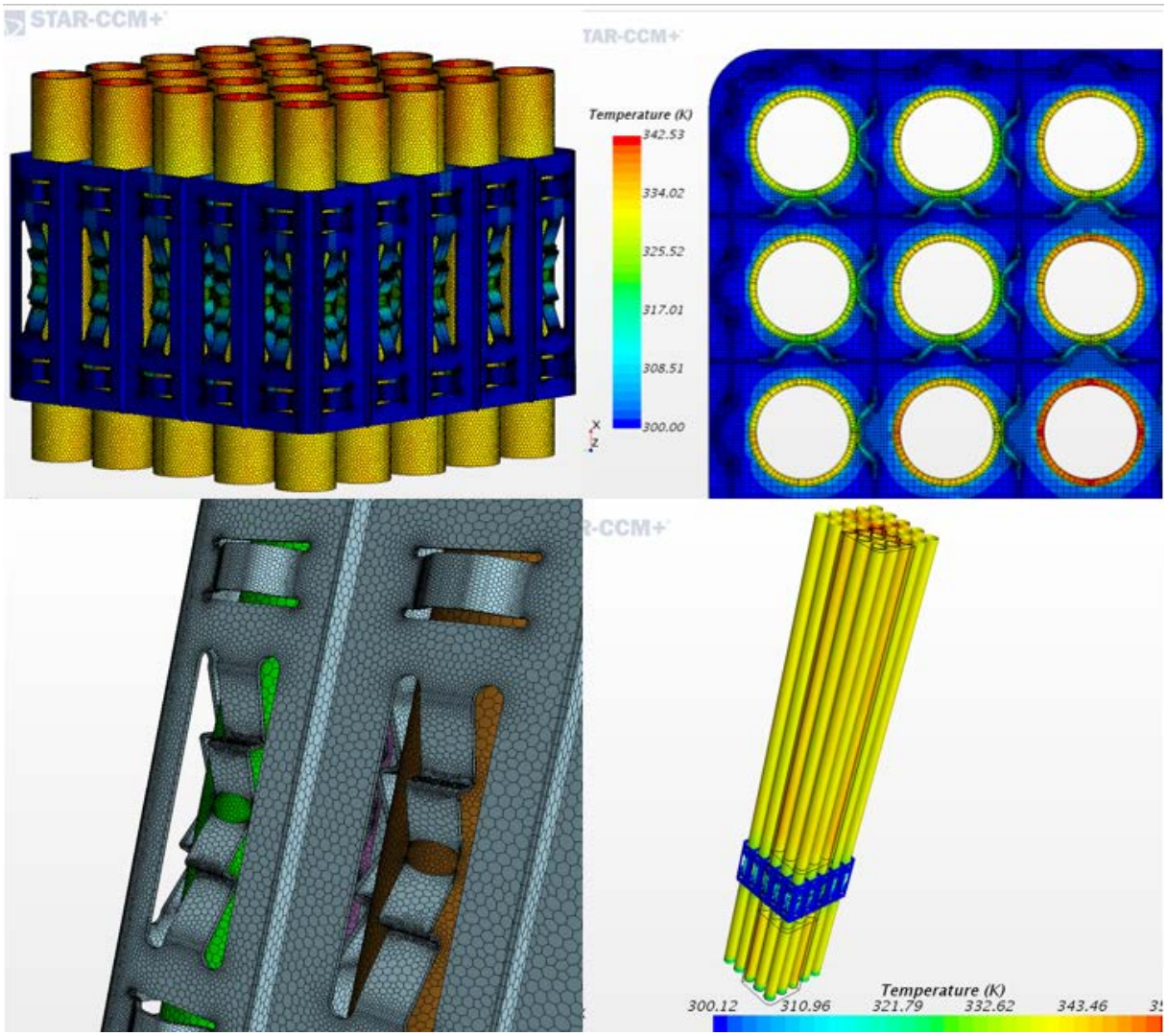

Figure 12 closer look on spacer grid mesh, and preliminary conjugate heat transfer results

5. Conclusions and Future works

The purpose of this study is to evaluate the DNB predictive capability of the Generation-I boiling model in the STAR-CCM+. The approach is assessed by comparing the simulated DNB results with existing experimental DNB datasets both qualitatively and quantitatively. The validated simulation approach leads to a best practice guideline for the DNB modeling in the nuclear thermal hydraulic application. The main results and key findings can be reiterated as follows:

- A subcooled flow boiling DNB calculation using a multiphase CFD approach is developed and tested.
- Full history-of-boiling curves and the DNB points for each test condition are calculated and compared with corresponding experimental DNB datasets.
- The trend behavior on the calculated DNB follows the general observations from experimental DNB literature.
- Parametric studies of microscopic boiling closure relation with varying operating condition are performed.

- The DNB calculated from the proposed CFD methodology shows an excellent agreement with independent experimental datasets (less than 20% deviation) over the range of the test conditions.

There are improvements to be made in the microscopic boiling closure model. In particular, the coupling between the microscopic closures and the macroscopic system response are significant areas for future improvement. Another important question for future work would be how variations in microscopic boiling closures relations systematically affect the macroscopic system response such as boiling curve and DNB.

6. References

1. S.J. Kim, L. Zou, B.G. Jones, "An experimental study on subcooled flow boiling CHF of R134a at low pressure condition with atmospheric pressure (AP) plasma assisted surface modification," *International Journal of Heat and Mass Transfer*, **81**, pp. 362-372 (2015).
2. S. Lo, "Application of population balance to CFD modeling of bubbly flow via the MUSIC model," AEA Technology, AEAT-1096 (1996).
3. G.H. Yeoh, J.Y. Tu, "A unified model considering force balances for departing vapor bubbles and population balance in subcooled boiling flow," *Nuclear Engineering and Design*, **235**, pp. 1251-1265 (2005).
4. B.J. Yun, A. Splawski, S. Lo., C.H. Song., "Prediction of a subcooled boiling flow with advanced two-phase flow models," *Nuclear Engineering and Design*, **253**, pp. 351-359 (2012).
5. E .Baglietto, "A New Approach to Subgrid Boiling Closures for CFD: towards the DNB Grand Challenge," Keynote paper at the 9th International Conference on Boiling and Condensation Heat Transfer, Boulder, CO, April 2015 (2015).
6. R.J.Weatherhead, "Nucleate boiling characteristics and the critical heat flux occurrence in subcooled axial-flow water systems," *AEC Research and Development Report*, ANL-6675 (1963).
7. E. Baglietto, M. Christon, "Demonstration & Assessment of Advanced Modeling Capabilities to Multiphase Flow with Sub-Cooled Boiling," CASL Technical Report: CASL-U-2013-0181-001, December 23, 2013 (2013).
8. A. Bui, N. Dinh, B. Williams, "Validation and calibration of nuclear thermal hydraulics multiscale Multiphysics models – subcooled flow boiling study," INL/EXT-13-30293 (2013).
9. M. Podowski, A. Alajbegovic, N. Kurul, "Mechanistic modeling of CHF in forced convection subcooled boiling," KAPL-P-000162 Report (1997).
10. D. Groenveveld, et al., "The 2006 CHF look-up table," *Nuclear Engineering and Design*, 237, pp. 1909-1922 (2007).
11. Description of Westinghouse Rod Bundle Test with NMV Grid Spacers, PFT-13-8, WEC DNB report